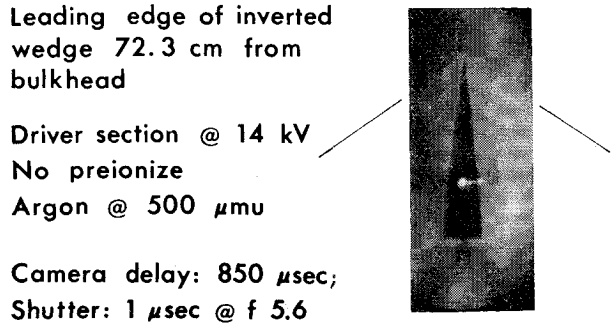

Fig. 2 Reflected wave enveloping inverted aerodynamic wedge.

both to improve with increasing pressure. The plasma homogeneity was good towards the front of the reflected wave but deteriorated somewhat toward the rear. With decreasing pressure, the length of the luminosity decreased while the homogeneity tended to improve.

At 570 μsec delay in Fig. 1, an intense luminosity stand-off may be seen in front of the reflecting bulkhead. Because in an EMST the temperature of the driver gas exceeds that of the driven gas,[2] this luminosity indicates the existence of an interaction zone and its extent after reflection. Intense luminosity stand-off was not observed during runs in which the pressure was less than 1000 μ, indicating the absence of an interaction zone at these pressures and confirming observations of others.[6,7]

The reflected wave was photographed, at shutter speeds of 1 μsec, as it enveloped an inverted aerodynamic wedge of half-angle 6.3°. Two series of runs were made with the wedge leading edge 72.3 cm from the bulkhead. Data from the first series (capacitor bank at 12 kv) indicated a region of constant Mach angle flow approximately 60 μsec long; however, the shock was not sharp and the Mach angle approached the largest allowable limit compatible with a wedge half-angle of 6.3°. The second series, with the wedge in the same position but the shock tube at 14 kv, indicated a constant Mach angle flow of 80 μsec duration, within an experimental accuracy of ±10 μsec. The Mach angle for this period was 54.24 ± 1.0°, and Fig. 2 is a typical of the data. Because the data from the second series of runs lies in a region of high shock-shape dependence, an error of 1° in the Mach angle would result in a Mach number error of order 0.025, if the gas remained at constant temperature.

A final two series of runs were performed with the wedge leading edge 40.2 cm from the bulkhead and the shock tube voltage at 12 kv and 14 kv, respectively. No shocks were observed in any of the data; which is not surprising since one of the boundary conditions is that the plasma velocity at the bulkhead be zero for all time.

Assuming an electrically neutral plasma in thermal equilibrium, an iterative procedure (to account for the variation of the ratio specific heats with temperature and pressure) involving the 54.25° Mach angle and plasma velocity was used to estimate the temperature of the reflected plasma. Since for this case, the luminous front velocity was 3500 m/sec the temperature was evaluated over a 3500–2500 m/sec plasma velocity range. The variation of temperature with velocity was almost linear and yielded for a velocity of 3500 m/sec, Mach 1.510, T = 13,430°K, and for a velocity of 2500 m/sec, Mach No. = 1.415, T = 11,000°K.

Discussion

Although at this time we propose no detailed mechanism to account for the markedly increased stability of the reflected wave, it appears likely to result from a reproducible energy addition followed by an inertially unstable expansion toward the bulkhead and, after compression against the bulkhead, an inertially stable expansion away from the bulkhead. It should be noted that, except in its early stages, the reflected wave propagates into the tail of the incident wave which, although probably still nonuniform is sufficiently rarefied that it has negligible effect upon the motion of the reflected wave.

A complimentary investigation of the temperature by a method independent of the shock shape, could be used to substantiate the shock shape data. Although such an investigation has not been performed, the present results are in good agreement with Makarov and Makismov's[5] measurements of the thermodynamic state behind the reflected shock in their conical EMST.

The blast wave reflection theory of Chang and Laporte[4] gives an analysis of the position of the reflected shock and the flow variables immediately either side of it. Although flow variables a finite distance from the shock were not given, the authors make the statement, "that in all probability, a reverse flow will be induced behind the reflected shock." If the flow in our EMST approximates that of a one-dimensional blast wave (with the exception of temperature), this research experimentally substantiates their findings.

Summary

Experimental evidence indicates that: 1) the plasma generated in an EMST is considerably more stable and uniform after reflection off a downstream bulkhead than it is as it initially moves away from the driver section, and that 2) there exists a reverse flow within the reflected plasma which under some circumstances is supersonic.

References

[1] Guthart, H. and Morita, T., "The Magnetic and Ionic Structure of an Electromagnetically Produced Shock," SRI TR 16, Jan. 1964, Stanford Research Institute, Menlo Park, Calif.

[2] Thornton, J. A., "A Spectroscopic Study of the Argon Plasmas Generated in a Conical Type Electromagnetic Shock Tube," NU-GDL Rept. B-2-63, June 1963, Gas Dynamics Lab., Northwestern University, Evanston, Ill.

[3] Scott, D. S., "Design and Performance of a Multicircuit Conical Electromagnetic Shock Tube," Mech. Eng. TP 6806, June 1968, University of Toronto.

[4] Chang, T. S. and Laporte, O., "Reflection of Strong Blast Waves," *The Physics of Fluids*, Vol. 7, No. 8, Aug. 1964, pp. 1225–1232.

[5] Makarov, Yu. V. and Makismov, A. M., "Investigation of Processes Behind a Reflected Shock Wave in an Electromagnetic Shock Tube," *Soviet-Physics Technical-Physics*, Vol. 11, No. 2, Aug. 1966, pp. 203–212.

[6] Cloupeau, M., "Interpretation of Luminous Phenomena Observed in Electromagnetic Shock Tubes," *The Physics of Fluids*, Vol. 6, No. 5, May 1963, pp. 679–688.

[7] Makarov, Yu. V. and Makismov, A. M., "Study of Luminescence Front Structure in Electromagnetic Shock Tubes," *Soviet-Physics Technical-Physics*, Vol. 10, No. 2, Aug. 1965, pp. 183–184.

Nonsimilar Behavior of Ablating Graphite Sphere Cones

EUGENE P. BARTLETT*
Aerotherm Corporation, Mountain View, Calif.

RESULTS obtained by the method of Ref. 1 are presented for the nonsimilar laminar chemically-reacting boundary layer over ablating graphite sphere cones under typical bal-

Received June 12, 1969; revision received February 24, 1970. This work was supported by U.S. Atomic Energy Commission under contract to Sandia Laboratories and Sandia contract to Aerotherm Corporation (Contract 6002-005).

* Manager, Aerochemistry Department, Analytical Services Division. Member AIAA.

Table 1 Nonsimilar ablation of graphite sphere cone: nose radius = 1 in., cone half-angle = 5°, surface emissivity = 1[a]

	Total enthalpy, Btu/lb				
	11,500	11,500	11,500	8,000	4,000
	Total pressure, atm				
	0.1	1	30	30	30
	a) Ablation rate, $\dot{m}_w$, lb/sec ft^2				
S/R_N	$\times 10^4$	$\times 10^3$	$\times 10^2$	$\times 10^2$	$\times 10^2$
0	88.29	48.73	41.70	31.45	18.01
0.375	77.33	41.46	36.91	27.71	15.87
0.687	54.91	24.37	25.28	18.68	11.09
1.004	33.46	9.114	12.79	9.120	5.773
1.211	21.20	4.186	6.020	4.103	3.312
1.484	9.940	2.353	0.569	0.549	1.536
1.585	8.435	2.010	−0.229	0.114	1.174
1.703	7.726	1.919	−0.243	0.357	1.119
2.470	5.716	1.563	0.053	0.530	0.834
4.030	3.875	1.122	0.276	0.504	0.616
7.283	2.411	0.732	0.299	0.386	0.426
12.954	1.597	0.501	0.242	0.279	0.315
	b) Surface temperature, T_w, °R				
0	5,649	6,792	8,137	7,937	7,234
0.375	5,523	6,703	8,063	7,861	7,143
0.687	5,144	6,462	7,880	7,670	6,936
1.004	4,551	6,045	7,578	7,348	6,529
1.484	3,358	4,559	6,842	6,453	5,252
1.703	3,161	4,278	6,662	6,080	4,893
2.470	2,928	3,940	6,212	5,536	4,506
4.030	2,653	3,556	5,574	4,960	4,118
7.283	2,351	3,142	4,860	4,375	3,719
12.954	2,116	2,823	4,334	3,992	3,424
	c) Blowing parameter,[b] B'				
0	0.2005	0.4011	0.7352	0.4928	0.2393
0.375	0.1936	0.3669	0.7177	0.4792	0.2330
0.687	0.1845	0.2897	0.6695	0.4416	0.2246
1.004	0.1828	0.2223	0.5854	0.3783	0.2057
1.484	0.1845	0.1853	0.3543	0.2315	0.1816
1.703	0.1841	0.1850	0.2780	0.2005	0.1821
2.470	0.1834	0.1853	0.2051	0.1902	0.1800
4.030	0.1840	0.1861	0.1873	0.1911	0.1811
7.283	0.1850	0.1869	0.1872	0.1957	0.1800
12.954	0.1862	0.1863	0.1895	0.2004	0.1800

[a] These results are based on laminar flow. Transition may occur on the conical portion in the 30 atm cases for which the $Re\theta$ is 250 at an S/R_N of about 3 and 300 at an S/R_N of about 12.
[b] The blowing parameter B' is based on $\rho_e U_e C_M$ as defined by Eq. (1).

listic entry conditions. The boundary layer is considered to be in equilibrium with the exception that condensation is not permitted within the boundary layer. The boundary layer is considered to be in equilibrium with the surface, and surface mass and steady-state energy balances are performed. Thus, the solutions provide predictions for steady-state ablation rates and surface temperatures as well as detailed boundary-layer characteristics. The purpose of this Note is to summarize these ablation-rate and surface-temperature results, emphasizing their nonsimilar behavior, and to correlate these results in terms of mass-transfer coefficients. Other details of the solutions can be found in Ref. 2.

Ablation rates and surface temperatures for a 1-in. nose radius, 5° cone half-angle are presented in Table 1, parts a and b, respectively, for several combinations of total enthalpy and total pressure. The ablation rates just aft of the sphere-cone juncture (S/R_N of the order of 1.5 to 2.0) are seen to dip well below values further back on the conical afterbody for the more severe conditions, even becoming negative (i.e., deposition) in one of the tabulated cases. This behavior is a direct consequence of the fact that carbon supplied from upstream is in excess of that needed to achieve surface equilibrium at downstream stations. In particular, surface temperatures in the stagnation region under the more severe conditions are sufficiently high that substantial carbon vapor is injected into the boundary layer, while temperatures at positions around the body become lower and permit less (and eventually no) carbon vapor at the surface (i.e., moving from the sublimation regime to the diffusion-controlled oxidation regime, see e.g., Ref. 3). Thus, some of the oxygen which diffuses across the boundary layer is predicted to react with carbon vapor supplied from upstream, thereby decreasing the amount of oxygen available to react with the wall.† The resultant dip in ablation rate is obviously a nonsimilar effect and could not be predicted by a similar boundary-layer technique such as that of Ref. 3.

In order to get a better appreciation for these nonsimilar ablation results, it is useful to correlate them in terms of locally similar transfer coefficient formulations. The nonsimilar effects can be absorbed into either the mass-transfer coefficient or into the driving potential for mass transfer. Both of these approaches are considered.

† In the event that the supply of carbon is more than can be accommodated by the available oxygen, the boundary layer is predicted to become supersaturated with carbon vapor, and deposition is predicted to occur at the wall. Alternatively, carbon particles might form in the boundary layer or at the surface and be swept downstream. Such alternative models have not been considered in the present study.

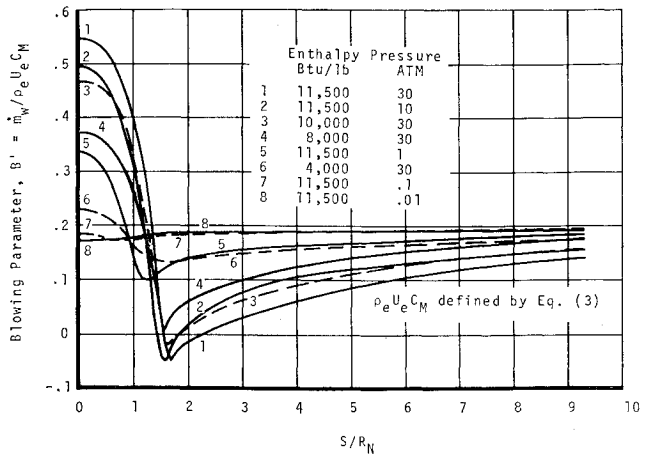

Fig. 1 Blowing parameter around a sphere cone for quasi-steady graphite ablation: $R_N = 1$ in., $\theta_c = 5°$, $\epsilon_w = 1.0$.

The first approach was investigated using the transfer coefficient formulation of Ref. 4, which employs a novel driving potential to account for unequal diffusion effects. In this approach, a mass-transfer coefficient for the kth element (irrespective of molecular configuration) is defined as

$$\rho_e U_e C_{M_k} = -\tilde{j}_{k_w}/(\tilde{Z}_{k_e}^* - \tilde{Z}_{k_w}^*) \quad (1)$$

where $\tilde{j}_k$ is the diffusive mass flux of element k away from the wall, the subscripts w and e refer to the wall and boundary-layer edge, respectively, and $\tilde{Z}_k^*$ is an elemental fraction (see Ref. 4) which, for unequal diffusion coefficients, is intermediate between a mass and a mole fraction. One of the purposes of the $\tilde{Z}_k^*$ potential is that the $\rho_e U_e C_{M_k}$ would hopefully be nearly the same for all elements k in unequal-diffusion similar‡ boundary-layer problems. It is shown in Refs. 5 and 6 that $\tilde{Z}_k^*$ performs this intended function well. Furthermore, there are only two effective components in the present problem,‡ air and carbon. Hence, a single $\rho_e U_e C_M$ can be considered to represent the $\rho_e U_e C_{M_k}$ for the present nonsimilar, unequal-diffusion boundary-layer solutions.

Correlating the nonsimilar boundary-layer results for $\tilde{j}_{k_w}$ and the $\tilde{Z}_k^*$ potential in terms of Eq. (1), the resulting $\rho_e U_e C_M$ were seen to have the same general behavior as the ablation rates (e.g., they become negative under the same conditions).[2] Furthermore, defining a blowing parameter in the conventional manner as the ratio of ablation rate to mass-transfer coefficient

$$B' \equiv \dot{m}_w/\rho_e U_e C_M \quad (2)$$

it can be seen from the results tabulated in Table 1, part c, that B' varies smoothly from the stagnation-point values to values representative of diffusion-controlled surface oxidation.

This result is a direct consequence of the definitions of $\rho_e U_e C_M$ and B'. With these definitions and considering elemental mass balances at the wall, it can be shown for the present problem that B' depends only upon the thermodynamic properties of the main stream, of the fluid in contact with the surface, and of the ablative substance and is, therefore, a function only of the boundary-layer edge gas, the surface material, pressure, and surface temperature and does not depend upon whether the boundary layer is similar or nonsimilar—any nonsimilar effect manifesting itself in the $\rho_e U_e C_M$.

Following the second approach where the primary nonsimilar effect is absorbed into the driving potential for mass transfer, one can demand that the $\rho_e U_e C_M$ be given by some convenient correlation expression such as

$$\rho_e U_e C_M = \rho_e U_e C_H (Le)^{2/3} \quad (3)$$

where Le is the system Lewis number defined in Ref. 4 and $\rho_e U_e C_H$ is a heat-transfer coefficient based on an equilibrium enthalpy potential. Utilizing values of Le§ and $\rho_e U_e C_H$ from the boundary-layer solution and $\rho_e U_e C_M$ and B' from Eqs. (3) and (2) yields the streamwise distributions for B' shown in Fig. 1. It can be seen that the nonsimilar ablation effect now manifests itself in B'. Computationally, in order to utilize this approach with a locally similar transfer-coefficient approach one could consider the composition of the edge gas to vary such as to yield values of B' consistent with the assumed values for $\rho_e U_e C_M$. That is, one could add carbon to the edge gas to simulate the fact that carbon is being supplied from upstream.

In summary, a dominant nonsimilar effect has been predicted to occur for ablating graphite sphere cones under ballistic entry conditions. This same effect is predicted for other carbon-containing ablation materials, but is not always so clearly evident. Secondly, two approaches for correlating these nonsimilar boundary-layer results with similar boundary-layer correlation procedures have been evaluated. It was seen that both approaches can be forced to work for the present problem; however these methods may have to be extended to deal with individual mass-transfer coefficients in order to have general applicability to nonsimilar boundary-layer problems. Perhaps the major conclusions should be that there is a potential for substantial nonsimilar events in boundary layers over ablating bodies and that the availability of codes such as that described in Ref. 1 makes it no longer necessary to ignore these effects. Also, more general transfer-coefficient formulations are needed for correlating nonsimilar boundary-layer solutions over ablating bodies for use in heat-shield design studies since it is often impractical to couple directly a nonsimilar boundary-layer procedure to a finite-difference transient heat conduction code.

‡ In nonsimilar boundary-layer problems, the $\rho_e U_e C_{M_k}$ will differ in general even for assumed equal diffusion coefficients if there are more than two effective components, namely if the elemental composition of the edge gas or injected material varies with streamwise position.

§ Nominally 1.00 for the present problem.

References

[1] Kendall, R. M. and Bartlett, E. P., "Nonsimilar Solution of the Multicomponent Laminar Boundary Layer by an Integral-Matrix Method," *AIAA Journal*, Vol. 6, No. 6, June 1968, pp. 1089–1097.

[2] Bartlett, E. P. and Grose, R. D., "The Multicomponent Laminar Boundary Layer over Graphite Sphere Cones: Solutions for Quasi-steady Ablation and Application to Transient Reentry Trajectories," Sandia Rept. SC-CR-68-3665, May 1968, Aerotherm Corp., Mountain View, Calif.

[3] Scala, S. M. and Gilbert, L. M., "Sublimation of Graphite at Hypersonic Speeds," *AIAA Journal*, Vol. 3, No. 9, Sept. 1965, pp. 1635–1644.

[4] Kendall, R. M., Rindal, R. A., and Bartlett, E. P., "A Multicomponent Boundary Layer Chemically Coupled to an Ablating Surface," *AIAA Journal*, Vol. 5, No. 6, June 1967, pp. 1063–1071.

[5] Bartlett, E. P. and Grose, R. D., "An Evaluation of a Transfer Coefficient Approach for Unequal Diffusion Coefficients," Sandia Rept. SC-CR-69-3270, June 1969, Aerotherm Corp., Mountain View, Calif.

[6] Grose, R. D. and Bartlett, E. P., "An Evaluation of a Transfer Coefficient Approach for Unequal Diffusion Coefficients," *AIAA Journal*, Vol. 8, No. 6, June 1970, to be published.